doi.org/10.26434/chemrxiv.12162360.v1

Homology Modeling and Docking Studies of TMPRSS2 with Experimentally Known Inhibitors Camostat Mesylate, Nafamostat and Bromhexine Hydrochloride to Control SARS-Coronavirus-2

Kailas Sonawane, Sagar S. Barale, Maruti J. Dhanavade, Shailesh R. Waghmare, Naiem H. Nadaf, Subodh A. Kamble, Ali Abdulmawjood Mohammed, Asiya M. Makandar, Prayagraj M. Fandilolu, Ambika S. Dound, Nitin M. Naik

Submitted date: 21/04/2020 • Posted date: 22/04/2020

Citation information: Sonawane, Kailas; Barale, Sagar S.; Dhanavade, Maruti J.; Waghmare, Shailesh R.; Nadaf, Naiem H.; Kamble, Subodh A.; et al. (2020): Homology Modeling and Docking Studies of TMPRSS2 with Experimentally Known Inhibitors Camostat Mesylate, Nafamostat and Bromhexine Hydrochloride to Control SARS-Coronavirus-2. ChemRxiv. Preprint. https://doi.org/10.26434/chemrxiv.12162360.v1

The rapid outbreak of SARS-Coronavirus 2 (SARS-CoV-2) caused a serious global public health threat. The spike ‘S’ protein of SARS-CoV-2 and ACE2 of the host cell are being targeted to design and discover new drugs to control Covid-19 disease. Similarly, a transmembrane serine protease, TMPRSS2 of the host cell has been found to play a significant role in proteolytic cleavage of viral spike protein priming to the receptor ACE2 present in human cell. However, three dimensional structure and inhibition mechanism of TMPRSS2 is yet to be explored experimentally. Hence, in the present study we have generated a homology model of TMPRSS2 and studied its binding properties with experimentally studied inhibitors viz. Camostat mesylate, Nafamostat and Bromhexine hydrochloride (BHH) using molecular docking technique. Docking analysis revealed that the Camostat mesylate and its structural analogue Nafamostat interacts strongly with residues His296, Ser441 and Asp435 present in catalytic triad of TMPRSS2. However, BHH interacts with Gln438 and other residues present in the active site pocket of TMPRSS2 through hydrophobic contacts effectively. Thus, these results revealed the inhibition mechanism of TMPRSS2 by known inhibitors Camostat mesylate, Nafamostat and Bromhexine hydrochloride in detail at the molecular level. However, Camostat mesylate shows strong binding as compared to other two inhibitors. This structural information could also be useful to design and discover new inhibitors of TMPRSS2, which may be helpful to prevent the entry to SARS-Coronavirus 2 in human cell.

File list (3)

Homology modeling and docking studies of TMPRSS2 with experimentally known inhibitors Camostat mesylate, Nafamostat and Bromhexine hydrochloride to control SARS-Coronavirus-2

Kailas D. Sonawane [a,b*], Sagar S. Barale [b], Maruti J. Dhanavade [b], Shailesh R. Waghmare [b], Naiem H. Nadaf [b], Subodh A. Kamble [a], Ali Abdulmawjood Mohammed [a], Asiya M. Makandar [b], Prayagraj M. Fandilolu [a], Ambika S. Dound [a], and Nitin M. Naik [b]

[a] Structural Bioinformatics Unit, Department of Biochemistry, Shivaji University, Vidyanagar, Kolhapur 416004, Maharashtra, India

[b] Department of Microbiology, Shivaji University, Vidyanagar, Kolhapur 416004, Maharashtra, India

Running Head: TMPRSS2 inhibition to control SARS-Coronavirus-2

*Corresponding author:

Prof. (Dr.) Kailas D. Sonawane
Professor and Coordinator
Structural Bioinformatics Unit
Department of Biochemistry,
Shivaji University,
Vidyanagar, Kolhapur (MS) 416004.
India.
E mail: kds_biochem@unishivaji.ac.in
Phone: +91-9881320719

Abstract

The rapid outbreak of SARS-Coronavirus 2 (SARS-CoV-2) caused a serious global public health threat. The spike 'S' protein of SARS-CoV-2 and ACE2 of the host cell are being targeted to design and discover new drugs to control Covid-19 disease. Similarly, a transmembrane serine protease, TMPRSS2 of the host cell has been found to play a significant role in proteolytic cleavage of viral spike protein priming to the receptor ACE2 present in human cell. However, three dimensional structure and inhibition mechanism of TMPRSS2 is yet to be explored experimentally. Hence, in the present study we have generated a homology model of TMPRSS2 and studied its binding properties with experimentally studied inhibitors *viz.* Camostat mesylate, Nafamostat and Bromhexine hydrochloride (BHH) using molecular docking technique. Docking analysis revealed that the Camostat mesylate and its structural analogue Nafamostat interacts strongly with residues His296, Ser441 and Asp435 present in catalytic triad of TMPRSS2. However, BHH interacts with Gln438 and other residues present in the active site pocket of TMPRSS2 through hydrophobic contacts effectively. Thus, these results revealed the inhibition mechanism of TMPRSS2 by known inhibitors Camostat mesylate, Nafamostat and Bromhexine hydrochloride in detail at the molecular level. However, Camostat mesylate shows strong binding as compared to other two inhibitors. This structural information could also be useful to design and discover new inhibitors of TMPRSS2, which may be helpful to prevent the entry to SARS-Coronavirus 2 in human cell.

Keywords: COVID-19, SARS-CoV-2, TMPRSS2, Homology modeling, Molecular docking.

Introduction

Currently, coronavirus is a major public health threat to the world, which is originated from Wuhan, Hubei Province, China in December, 2019. Earlier outbreaks caused by coronavirus are known as Severe Acute Respiratory Syndrome (SARS-CoV) and Middle East Respiratory Syndrome (MERS-CoV). But the outbreak caused in 2019 by SARS-CoV-2 is novel and named as COVID-19 by WHO [1]. As on 1st April, 2020 more than 195 countries have been affected by this novel coronavirus-2. After China, the European countries and America are affected severely with more mortality rates in the Italy. The incubation period of COVID-19 is approximately 5.2 days [2], but it is shorter in elderly patients (age >70) [3]. The most common symptoms after the onset of COVID-19 infection are cough, fever and fatigue, while other symptoms include headache, sputum production, diarrhea, haemoptysis, lymphopenia and dyspnoea [3-6]. The study suggests that COVID-19 originated from wet market of Wuhan city, but it has transmitted primarily by person-to-person contacts or through droplet nuclei formed after coughing or sneezing [7].

SARS-CoV-2 is an enveloped virus with positive sense RNA genome, belongs to family Coronaviridae of the order Nodovirales and genera Betacoronavirus [8]. Recently it has been shown that SARS-CoV-2 enters in the host cell by interacting its spike glycoprotein and receptor present on epithelial cells i.e. Angiotensin Converting Enzyme-2 (ACE-2) [9]. The highest expression of ACE-2 has been observed in lungs, kidneys and heart cells [10-11], so the most of the fatalities observed due to damage of lungs. Efforts are being made to develop an effective vaccine to control pandemic of SARS-CoV-2, but they are time consuming and might require more clinical trials to come into the market. Development of vaccine against SARS-CoV-2 is also difficult due to mutation in spike glycoprotein of corona virus. In vitro study is reported on Nafamostat, a inhibitor of serine protease TMPRSS2 to block MERS-CoV infection [12]. Similarly, bromhexine hydrochloride an ingredient in a mucolytic cough suppressant could also be used for the treatment of influenza virus and coronavirus infections as inhibitor of TMPRSS2 [13]. However, few potential targets for the treatment of influenza virus and coronavirus infections have been summarized earlier [14]. Steardo et al 2020 reported that the Coronavirus can infect the brain cells resulting in more complex clinical scenario [15].

As the virus is novel, so no authenticated full proof remedies are available to control the SARS CoV-2, but currently various broad spectrum antiviral drugs are being used to treat COVID-19 patients, where as antimalarial drugs i.e. Chloroquine and its derivative hydroxychloroquine have also shown positive effects to control the infection [16]. The glycosylated spike 'S' protein of SARS-CoV-2 and ACE2 of the host cell have been studied thoroughly [17-18] and would be useful to design and discover new lead molecules to control the SARS-CoV-2. The another drug target *i.e.* the transmembrane serine protease (TMPRSS2) of the host cell can act proteolytically to cleave viral spike 'S' protein which is useful for the priming to the receptor ACE2 present in host cell [19-20]. The excellent work by Haffman and coworkers, 2020, suggested that influenza virus and coronavirus infections can be controlled by targeting the host cell protease, TMPRSS2 [21]. So the inhibition of TMPRSS2 could be a promising therapy to control viral entry into the human cell.

However, there is no literature available about the three-dimensional structure of TMPRSS2 and its inhibition mechanism by various inhibitors. Hence, in the present study, we have generated a three-dimensional model of TMPRSS2 using homology modeling technique. Further, this model was considered to investigate the interactions between TMPRSS2 and experimentally approved inhibitors such as Camostat mesylate, Nafamostat and Bromhexine hydrochloride using molecular docking technique. Molecular docking analysis revealed that the Camostat mesylate, Nafamostat and Bromhexine hydrochloride interacts with residues present active site pocket of TMPRSS2. Thus, this structural information of TMPRSS2 could be useful to design new lead molecules to control the novel coronavirus-2 entry into the human cells.

Material and methods

Sequence retrieval and Homology modeling of TMPRSS2

Amino acid sequence of transmembrane serine protease TMPRSS2 (Accession No C9JKZ3) has been extracted from Uniprot [22]. Further, we searched the suitable template to build a homology model of TMPRSS2 using BLAST program [23]. Homology modeling of TMPRSS2 was done using online server PRIMO [24]. The three dimensional structure of TMPRSS2 was predicted by using template human plasma kallikrein (5TJX.pdb) [25]. Then the predicted model was refined by using ModRefiner [26]. The refined model of TMPRSS2 was validated using different online servers such as PROSA [27], PROCHECK [28] and PDBsum [29]. Finally, the verified

homology model of TMPRSS2 with good quality was further used for molecular docking studies.

Preparation and parameterization and inhibitors:

Three dimensional co-ordinates for Camostat mesylate (CID5284360), Nafamostat (CID4413) and Bromhexine hydrochloride (CID5702220) were extracted from Pubchem Database (https://pubchem.ncbi.nlm.nih.gov/) in sdf format and then converted into PDB format with the help of Open Babel [30]. DockPrep tool of chimera was used to prepare molecule for docking [31].

Prediction of binding pocket of TMPRSS2:

Computed Atlas of Surface Topography of proteins CASTp [32] online server was used to binding pocket on TMPRSS2, potential binding pocket were selected based on consensus of residues present in related serine proteases.

Molecular docking of TMPRSS2 with its inhibitors

Molecular docking

Molecular docking of homology model of TMPRSS2 with Camostat mesylate was performed using online docking server "Achilles", a blind docking server (uses Autodock vina) available at: http://bio-hpc.eu/software/blind-docking-server/. Protein model i.e. TMPRSS2 as a receptor and Camostat mesylate in pdb format separately sent to server to perform docking calculations. Series of docking calculations were performed across the whole protein in order to find binding sites, and results were clustered by using pose clustering algorithm.

Molecular docking by AutoDock

Homology modelling and molecular docking techniques have been found useful to investigate folding pattern and molecular interactions between several enzymes and ligands [33-42] Binding affinities of Camostat mesylate, Nafamostat and Bromhexine hydrochloride to the active site of modelled protein, TMPRSS2 were confirmed by Autodock 4.2 computational tool with Lamarckian Genetic Algorithm (LGA) [43]. Here, also blind docking was performed by taking protease domain in grid box. All residues in TMPRSS2 were kept as rigid. Grid dimensions were set to 60 Å × 60 Å × 60 Å to accommodate the ligand with 0.375 Å grid spacing. Grid centre was selected at X = 37.216 Y = 2.359 Z = 24.602 coordinates with 0.02 rate of mutation & 0.8 crossing over rate. Population size was fixed to 150 to generate 50 conformations for 27000

generations and for 25000 evaluations. The best docked complex was clustered on the basis of default RMSD tolerance range of 2.0 Å. Inhibition constant (Ki) of best docked pose was evaluated using in-built program of AutoDock. Ligand-receptor interactions were visualized with AutoDock and UCSF chimera [31].

Results and discussion

Homology evaluation and structural analysis of TMPRSS2:

Analysis of homology model of TMPRSS2

The three dimensional structure of TMPRSS2 (Accession No C9JKZ3) with 489 amino acid was predicted by using template human plasma kallikrein (5TJX.pdb). The template showed 42.56% identity with TMPRSS2 sequence. TMPRSS2 consists of intracellular domain (residues 1 to 84), transmembrane spanning domain (residues 84-106), low-density lipoprotein receptor domain (LDLRA: residues 133-147). The homology model of TMPRSS2 showed two extracellular domains; cysteine rich domain (residues 148-242) and serine protease domain (residues 255-489) (Figure 1). The residues His296, Asp345 and Ser441 are present as a catalytic triad in TMPRSS2 model (Figure 1). The CATSp analysis showed His296, Asp345 and Ser441 amino acid residues at the binding pocket along with several other residues (Figure 2). Model of TMPRSS2 was subjected to model refinement and energy minimization by online server ModRefiner [26]. Then predicted model was assessed by various online servers. The PROSA [27] analysis showed that the predicted model of TMPRSS2 has Z score of -7.48 (Figure 3A) as compared to template having Z score of -6.64 (Supplementary Figure 1). Also, most of the amino acid residues in the TMPRSS2 model showed negative interaction energy suggesting good quality of predicted structure (Figure 3B). To check the predicted model quality for TMPRSS2, we have further performed PROCHECK [28] analysis. This analysis shows that total 99% residues are present in allowed regions and only 1% residues in disallowed region (Figure 3 C) suggesting a good quality of TMPRSS2. There are various inhibitors of TMPRSS2 such as Camostat mesylate, Nafamostat and Bromhexine hydrochloride (Figure 4). These inhibitors are further used for molecular docking studies with predicted model of TMPRSS2 (Figure 1 and 2).

Active site prediction

Active site of serine proteases generally consists of SER, HIS, and ASP residues as catalytic triad [44]. Active site residues of TMPRSS2 were predicted by CASTp online server [32]. The results given by CASTp server showed that TMPRSS2 having several binding pockets, out of which 3 binding pockets contains at least one residue from the catalytic triad. As TMPRSS2 is a serine protease, hence pockets containing Ser, Thr, His, Asp residues, were selected for further study. However, from the selected pockets, we found that His296, Glu299, Asp435, Gln438, Ser441, Asp345, Ser346, Thr459, Ser460, Thr461 residues would also be useful for the TMPRSS2 activity (Supplementary Figure 2).

Binding interactions of TMPRSS2 with inhibitors in docked complex:

Initially binding sites of Camostat mesylate, Nafamostat and Bromhexine hydrochloride with TMPRSS2 were not known; hence blind docking was performed by online blind docking server. For the inhibitor Camostat mesylate, we obtained total 17 possible clusters of binding poses. Out of this -8.5 kcal/mole is a lowest binding energy pose with His296 and Ser441 as active residues, which is also predicted by CASTp server. The residues Ser441, His296, Glu299, Asp435, Val473 can form hydrogen bonds; whereas Val28, Asp440, Thr459, Ser460, Trp461, Tyr474 are also involved in Van der Waals interactions (Supplementary Figure 3). The molecular docking study revealed that Camostat mesylate can fit inside the pocket present in serine protease domain of TMPRSS2 and shown in different confirmations (Figure 5). The docked complex of TMPRSS2 with inhibitor Nafamostat, a structural analogue of Camostat mesylate also showed hydrogen bonding interactions (Figure 6A, Table 1). Bromhexine hydrochloride interacts with Gln438, whereas Nafamostat shows hydrogen bonding with Asp435, Gly464 and Ser441 of TMPRSS2 (Figure 6, Table 1). Docked complex analysis revealed that Camostat mesylate and Nafamostat binds in the same pocket of TMPRSS2.

The docked complex analysis of Bromhexine hydrochloride (BHH) with TMPRSS2 shows fewer hydrogen bonding interactions as compared to Camostat mesylate and Nafamostat (Table 2). Bromine atom of BHH interacts with Gln438 of TMPRSS2 (Figure 6C; Table 2). However, the residues such as His279, Val280, Cys281, and His296 of TMPRSS2 are providing additional hydrophobic interactions (Figure 6, Table 2). The docked complex of TMPRSS2 with Camostat mesylate showed that there is strong hydrogen bonding interaction between the different groups of Camostat mesylate with active site residues present in the catalytic triad such

as His296 and Ser441 (Figure 6 and Table 1). The Ser441 of TMPRSS2 interacts with Camostat mesylate carbon atom with strong interatomic distance of 2.232 Å. Similarly, other interacting residues of TMPRSS2 like Glu299, Thr459, Tyr474, Asp435, Ser436 and Gln438 also showed hydrogen bonding ability, hence these interactions can stabilize the Camostat mesylate into the binding pocket present in serine protease domain of TMPRSS2 (Figure 6 and Table 1).

The binding energy of TMPRSS2 with Camostat mesylate, Nafamostat and Bromhexine hydrochloride found to be -7.94, -7.21 and -5.96 respectively (Table 3). Similarly, the inhibitor constant (Ki) of these Camostat mesylate, Nafamostat and Bromhexine hydrochloride are 1.51 uM, 5.17 uM and 43 uM respectively as shown in Table 2. Overall, Camostat mesylate, Nafamostat and Bromhexine hydrochloride found to be good inhibitors of TMPRSS2. The interactions of Camostat mesylate, Nafamostat and Bromhexine hydrochloride may prevent the priming ability of transmembrane serine protease TMPRSS2 to activate the viral 'S' protein to the receptor ACE2 to facilitate the entry of SARS-CoV-2 in human cell. However, further clinical studies are necessary.

Conclusion:

Understanding effective drug target in detail at the molecular level becomes pivotal to combat SARS-CoV-2 infection. Hence, in the present study we predicted three dimensional structure of TMPRSS2 by using homology modeling technique and studied its interactions with known inhibitors with the help of molecular docking. The homology model of TMPRSS2 shows proper folding pattern with cysteine rich and serine protease domains. The docked complex revealed that the active site residues His296 and Ser441 of TMPRSS2 interact with the inhibitors Camostat mesylate and Nafamostat by proper hydrogen bonding interactions, whereas Bromhexine hydrochloride shows hydrophobic contacts because of its small structure.

However, camostat mesylate shows strong inhibition of TMPRSS2 as compared to nafamostat and bromhexine hydrochloride (Figure 6; Table 2 and 3). Therefore, these inhibitors *viz.* Camostat mesylate, Nafamostat and Bromhexine hydrochloride could be considered for the inhibition of TMPRSS2 a transmembrane serine protease to control the COVID-19 disease. Finally, the structural information obtained from the present study could be useful to design new approaches to control the coronavirus outbreak.

Acknowledgements:

KDS gratefully acknowledges DST-SERB, New Delhi for financial support (Ref. No. EMR/2017/002688/BBM dated 25th October 2018). KDS is also thankful to University Grants Commission, New Delhi for financial support under the UGC-SAP-DRS Phase-II scheme sanctioned to Department of Biochemistry, Shivaji University, Kolhapur. Authors thankfully acknowledge Department of Science and Technology, Government of India, New Delhi for financial support through DST-PURSE-Phase II (Ref no. SR/PURSE-PHASE-II/24(C) dated 8/3/2018]. Authors are very grateful to the Structural Bioinformatics unit, Department of Biochemistry, Shivaji University, Kolhapur and Department of Microbiology, Shivaji University, Kolhapur and for extending the laboratory facilities to complete the investigation. SSB is thankful to SARTHI for providing fellowship. All authors are thankful to Computer centre, Shivaji University, Kolhapur for providing necessary computational facilities.

Author contributions

Conceptualization: KDS.

Formal analysis: KDS, SSB, MJD.

Investigation: KDS, SSB, MJD.

Methodology: KDS, SSB, MJD, PMF, SAK, AAM, AMM, ASD, NMK.

Project administration: KDS.

Supervision: KDS.

Validation: KDS, SSB, MJD.

Writing ± original draft: KDS, SSB, MJD, SRW, NHN.

Writing ± review & editing: KDS, SSB, MJD, SRW.

Financial & competing interests disclosure: NA

References

1 Zhao S, Lin Q, Ran J, Musa S, Yang G, Wang W, et al., Preliminary estimation of the basic reproduction number of novel coronavirus (2019-nCoV) in China, from 2019 to 2020: a data-driven analysis in the early phase of the outbreak, *Int. J. Infect. Dis. : IJID : Off. Publ. Int. Soc. Infect. Dis.* 92, 214–217. (2020).

2 Li Q, Guan X, Wu P, Wang X, Zhou L, Tong Y, et al., Early transmission dynamics in wuhan, China, of novel coronavirus-infected pneumonia, *N. Engl. J. Med*. 382, 1199-1207. (2020).

3 Wang W, Tang J, Wei F. Updated understanding of the outbreak of 2019 novel coronavirus (2019-nCoV) in Wuhan, China, *J. Med. Virol.* 92(4), 441–447. (2020).

4 Ren L, Wang Y, Wu Z, Xiang Z, Guo L, Xu T, et al. Identification of a novel coronavirus causing severe pneumonia in human: a descriptive study, *Chinese Med J* doi: 10.1097/CM9.0000000000000722. (2020).

5 Huang C, Wang Y, Li X, Ren L, Zhao J, Hu Y, et al. Clinical features of patients infected with 2019 novel coronavirus in Wuhan, China, *Lancet* 395 (10223), 497–506. (2020).

6 Carlos W, Dela Cruz C, Cao B, Pasnick S, Jamil S. Novel wuhan (2019-nCoV) coronavirus, *Am. J. Respir. Crit. Care Med.* 201 (4), 7–8. (2020).

7 Rothan H, Byrareddy S. The epidemiology and pathogenesis of coronavirus disease (COVID-19) outbreak. *J. Autoimmun.* doi.org/10.1016/j.jaut.2020. 102433. (2020).

8 Seah I, Su X, Lingam G. Revisiting the dangers of the coronavirus in the ophthalmology practice. *Springer Nature.* doi.org/10.1038/s41433-020-0790-7. (2020).

9 Wu C., Liu Y, Yang Y, Zhang P, Zhong W, Wang Y, Wang Q, Xu Y, Li M, Li X, Zheng M, Chen L, Li H. Analysis of therapeutic targets for SARS-CoV-2 and discovery of potential drugs by computational methods. *Acta Pharm. Sin. B.*, https://doi.org/10.1016/j.apsb.2020.02.008. (2020).

10 Donoghue M, Hsieh F, Baronas E et al. A novel angiotensin-converting enzyme-related carboxypeptidase (ACE2) converts angiotensin I to angiotensin 1–9, *Circ. Res.* 87(5), E1–E9. (2000).

11 Tipnis S, Hooper N, Hyde R, Karran E, Christie G, Turner A. A human homolog of angiotensin converting enzyme: cloning and functional expression as a captopril-insensitive carboxypeptidase, *J Biol. Chem.* 275(43), 33238–33243. (2000).

12 Yamamoto M, Matsuyama S, Li X, Takeda M, Kawaguchi Y, Inoue J, Matsuda Z. Identification of nafamostat as a potent inhibitor of Middle East Respiratory Syndrome Coronavirus S protein-mediated membrane fusion using the split-protein-based cell-cell fusion assay, *Antimicrob. Agents. Chemother.* 60:6532e6539. (2016).

13 Lucas J, Heinlein C, Kim T, Hernandez S, Malik M, True L, Morrissey C, Corey E, Montgomery B, Mostaghel E, Clegg N, Coleman I, Brown C, Schneider E, Craik C, Simon J, Bedalov A, Nelson P. The androgen-regulated protease TMPRSS2 activates a proteolytic cascade involving components of the tumor microenvironment and promotes prostate cancer metastasis, Cancer Dis. 4, 1310e1325. (2014).

14 Shen LW, Mao HJ, Wu YL, Tanaka Y, Zhang W. TMPRSS2: A potential target for treatment of influenza virus and coronavirus infections, *Biochimie.* 142, 1-10. (2017).

15 Steardo L, Steardo Jr L, Zorec R, Verkhratsky A. Neuroinfection may potentially contribute to pathophysiology and clinical manifestations of COVID-19. *Acta. Physiol,* doi:10.1111/APHA.13473. (2020).

16 Touret F, de Lamballerie X. Of chloroquine and COVID-19. *Antivir. Res.* 177, 104762. (2020).

17 Senathilake K, Samarakoon S, Tennekoon K. Virtual screening of inhibitors against spike glycoprotein of 2019 novel corona virus: a drug repurposing approach, doi:10.20944/preprints202003.0042.v1. (2020).

18 Xia S, Liu M, Wang C, Xu W, Lan Q, Feng S, Qi F, Bao L, Du L, Liu S, Qin C, Sun F, Shi Z, Zhu Y, Jiang S and Lu L. Inhibition of SARS-CoV-2 (previously 2019-nCoV) infection by a highly potent pan-coronavirus fusion inhibitor targeting its spike protein that harbors a high capacity to mediate membrane fusion, *Cell Res.* 30, 343–355; https://doi.org/10.1038/s41422-020-0305-x. (2020).

19 Glowacka I, Bertram S, Muller M, Allen P, Soilleux E, Pfefferle S, Steffen I, Tsegaye T, He Y, Gnirss K. et al. Evidence that TMPRSS2 activates the severe acute respiratory syndrome coronavirus spike protein for membrane fusion and reduces viral control by the humoral immune response. *J Virol.* 85, 4122–4134. (2011).

20 Shulla A, Heald-Sargent T, Subramanya G, Zhao J, Perlman S, Gallagher T. A transmembrane serine protease is linked to the severe acute respiratory syndrome coronavirus receptor and activates virus entry. *J Virol.* 85, 873–882. (2011).

21 Hoffmann M, Kleine-Weber H, Schroeder S, Muller M, Drosten C, Pohlmann S. SARS-CoV-2 Cell Entry Depends on ACE2 and TMPRSS2 and Is Blocked by a Clinically Proven Protease Inhibitor, *Cell* 181, 1–10. (2020).

22 The UniProt Consortium, UniProt: a worldwide hub of protein knowledge, *Nucleic Acids Res.* 47, D506-515. (2019).

23 Altschul S, Gish W, Miller W, Myers E, Lipman, D. Basic local alignment search tool. *J Mol. Biol.* 215, 403-410. (1990).

24 Hatherley R, Brown D, Glenister M, Tastan Bishop Ö. "PRIMO: An Interactive Homology Modeling Pipeline." *PLoS One.* 17:11(11):e0166698. doi: 10.1371/journal.pone.0166698. (2016).

25 Partridge J, Choy R, Li Z. Structure of human plasma kallikrein. DOI: 10.1021/acsmedchemlett.6b00384, (2016).

26 Xu D. and Zhang Y. Improving the Physical Realism and Structural Accuracy of Protein Models by a Two-step Atomic-level Energy Minimization. *Biophysical J.* 101, 2525-2534. (2011).

27 Wiederstein M, Sippl M. ProSA-web: interactive web service for the recognition of errors in three-dimensional structures of proteins, *Nucleic Acids Res.* 35, W407–W410. (2007).

28 Laskowaski R, McArther M, Moss D, Thornton J. PROCHECK a program to check sterio-chemical quality of a protein structures, *J. Appl. Crystallogr.*, 26, 283–291. (1993).

29 Laskowski R, Jabłońska J, Pravda L, Vařeková R, Thornton J. PDBsum: Structural summaries of PDB entries, *Protein Sci.* 27(1), 129–134. (2018).

30 O'Boyle M, Banck M, James C, Morley C, Vandermeersch T, Hutchison G. Open Babel: An Open Chemical Toolbox. *J Cheminformatics.*, 3, 1–14. https://doi.org/10.1186/1758-2946-3-33. (2011).

31 Pettersen E, Goddard T, Huang C, Couch G, Greenblatt D, Meng E, Ferrin T. UCSF Chimera—a visualization system for exploratory research and analysis, *J Comput. Chem.*, 25, 1605–1612. (2004).

32 Tian et al., *Nucleic Acids Res.* PMID: 29860391 DOI: 10.1093/nar/gky473. (2018)

33 Jalkute C, Barage S, Dhanavade M, Sonawane K. Identification of Angiotensin Converting Enzyme Inhibitor: An In Silico Perspective, *Int J Pept Res Ther.*, 21, 107–115. (2015).

34 Jalkute C, Barage S, Dhanavade M, Sonawane K. Molecular Dynamics Simulation and Molecular Docking Studies of Angiotensin Converting Enzyme with Inhibitor Lisinopril and Amyloid Beta Peptide. Protein J, 32, 356-364. (2013).

35 Barage S, Jalkute C, Dhanavade M, Sonawane K. Simulated interactions between Endothelin converting enzyme and Aβ peptides: insights into subsite recognition and cleavage mechanism, *Int J Pept Res Ther*, 20, 409–420. (2014).

36 Dhanavade M, Parulekar R, Kamble S and Sonawane K. Molecular modeling approach to explore the role of cathepsin B from Hordeum vulgare in the degradation of Aβ peptides. *Mole. Biosys.*, 12, 162-168. (2016).

37 Dhanavade M, Sonawane K. Insights into the molecular interactions between aminopeptidase and amyloid beta peptide using molecular modeling techniques. *Amino Acids*, 46, 1853–1866. (2014).

38 Dhanavade M, Jalkute C, Barage S, Sonawane K. Homology modeling, molecular docking and MD simulation studies to investigate role of cysteine protease from Xanthomonas campestris in amyloid beta degradation. *Comput Biol Med.* 43, 2063–2070. (2013)

39 Parulekar R, Barage S, Jalkute C, Dhanavade M, Sonawane K. Homology modeling, molecular docking and DNA binding studies of nucleotide excision repair UvrC protein from M. Tuberculosis, *Protein*, 32, 467-476. (2013).

40 Sonawane K, Dhanavade M. Molecular docking technique to understand enzyme-ligand Interactions" Published in book "Methods and Algorithms for Molecular Docking-Based Drug Design and Discovery" *IGI Global*, Chapter 10, 245-264. (2015).

41 Sonawane K, Dhanavade M. "Computational Approaches to Understand Cleavage Mechanism of Amyloid Beta (Aβ) Peptide" Published in book "Computational Modeling of Drugs Against Alzheimer"s Disease" *Springer Neuromethods*, Chapter 11, 263282. (2017).

42 Barale S, Parulekar R, Fandilolu P, Dhanavade M, Sonawane K. Molecular Insights into Destabilization of Alzheimer's Aβ Protofibril by Arginine Containing Short Peptides: A Molecular Modeling Approach, *ACS Omega* 4(1), 892-903. (2019).

43 Morris G, Huey R, Lindstrom W, Sanner M, Belew R, Goodsell D. Olson A. AutoDock4 and AutoDockTools4: Automated Docking with Selective Receptor Flexibility. *J Comput Chem.* 30, 2785-91. https://doi.10.1002/jcc.2125. (2009).

44 Hedstrom L. Serine Protease Mechanism and Specificity, *Chem. Rev.* 102, 12, 4501-4524. (2002).

Figure Legends:

Figure 1: Predicted model of TMPRSS2 showing SRCR: Scavenger receptor cysteine rich domain (magenta) and catalytic triad HIS296, ASP345, and SER441 (orange) in serine protease domain (blue).

Figure 2: Predicted binding pocket by CATSp showing active site residues in orange.

Figure 3: PROSA analysis of TMPRSS2 model A) Z Score, B) Local model quality. C) Ramchandran plot of TMPRSS2 model.

Figure 4: Three dimensional structure of TMPRSS2 inhibitors Camostat mesylate (Magenta:L1), Nafamostat (green:L2) and Bromhexine hydrochloride (purple:L3).

Figure 5: Binding of Camostat mesylate (Magenta) with TMPRSS2 (Light sea green) inside its pocket shown in surface (A) and Atoms/Bonds type (B). Binding of Camostat mesylate (Magenta) with active site residues (Yellow) of TMPRSS2 (Light sea green) inside its pocket shown in surface.

Figure 6: Docking interaction of active site residues of TMPRSS (Yellow) with A) Camostat mesylate (Magenta) B) Nafamostat (green) C) Bromhexine hydrochloride (purple) and showed in Atoms/Bonds type. D) Super imposition of docked complex of all three inhibitor showing Camostat mesylate (Magenta), Nafamostat (green) and Bromhexine hydrochloride (purple) within active site of TMPRSS2 active site residues (Yellow).

Table Legends:

Table 1: Hydrogen bonding interactions between TMPRSS2 and different inhibitors.

Table 2: Molecular docking of TMPRSS2 with different inhibitors.

Table 1: Hydrogen bonding interactions between TMPRSS2 and different inhibitors.

Sr. No.	**Interactions between active site residues of TMPRSS2 with Camostat mesylate.**	**Distance in Å**
1	ASP 435 OD2---------- Lig. 1.A H	2.176
2	SER 441 HN ---------- Lig. 1.A O	3.061
3	VAL 473 O ---------- Lig. 1.A H	2.079
4	TYR 474 OH ---------- Lig. 1.A H	2.947
5	GLN 438 OE1---------- Lig. 1.A O	2.881
6	GLN 438 2HE2-------- Lig. 1.A O	2.450
7	HIS 296 HE2 ---------- Lig. 1.A C	2.855
8	GLU 299 OE2 ---------- Lig. 1.A O	3.143
9	SER 441 HG ---------- Lig. 1.A C	2.232
10	THR 459 CG2 ---------- Lig. 1.A C	2.952
11	SER 436 CB ---------- Lig. 1.A N	3.035
Sr. No.	**Interactions between active site residues of TMPRSS2 with Nafamostat.**	**Distance in Å**
1	SER 441 HG ---------- Lig. 2.A O	2.54
2	ASP 435 OD1 --------- Lig. 2.A H	2.18
3	ASP 435 OD2---------- Lig. 2.A H	2.55
4	GLY 464 O ----------Lig. 2.A H	2.28
Sr. No.	**Interactions between active site residues of TMPRSS2 with Bromhexine hydrochloride.**	**Distance in Å**
1	GLN 438 OE1 ----------Lig. 2.A BR	2.87
2	GLN 438 OE1 ---------- Lig. 2.A H	1.99

Table 2: Molecular docking of TMPRSS2 with different inhibitors.

Sr. No.	**NAME of Molecule**	**CID**	**Binding Energy (Kcal/mol)**	**Ki**
1	Camostat mesylate	5284360	-7.94	1.51 uM
2	Nafamostat	4413	-7.21	5.17 uM
3	Bromhexine hydrochloride	5702220	-5.96	43.00 uM

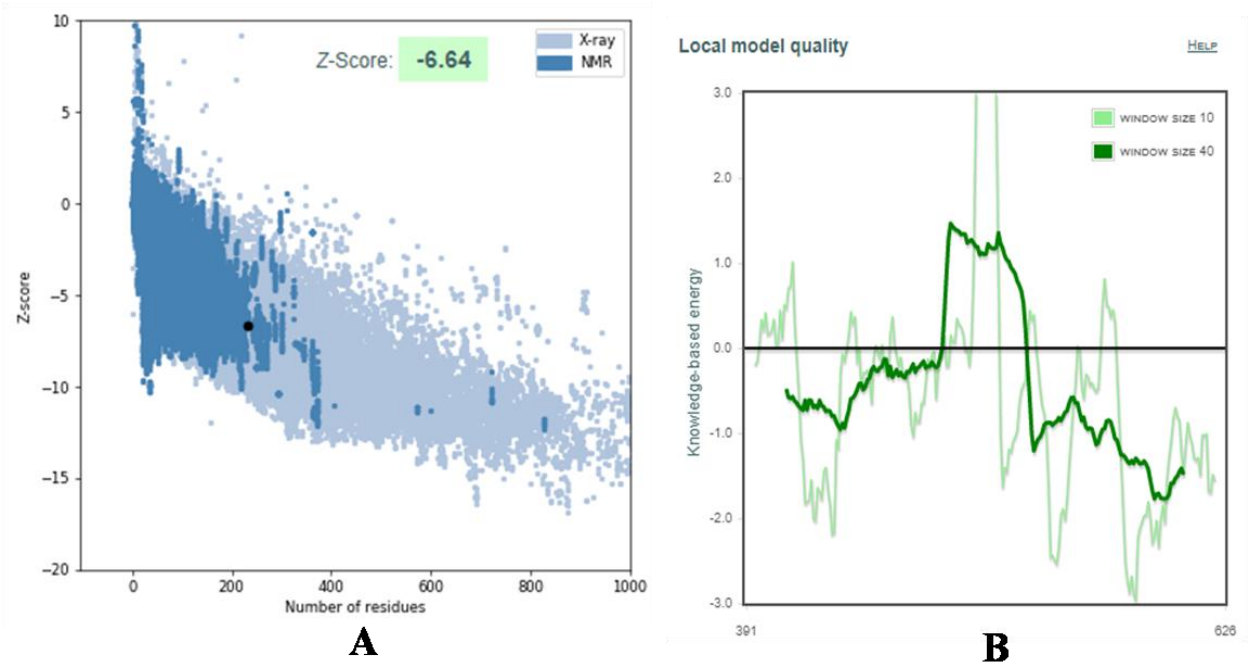

Supplementary figure 1: PROSA analysis of template A) Z Score, B) Local model quality.

Pocket 1

Pocket 2

Pocket 5 show targeted catalytic residues

Supplementary figure 2: Active site prediction using CastP server.

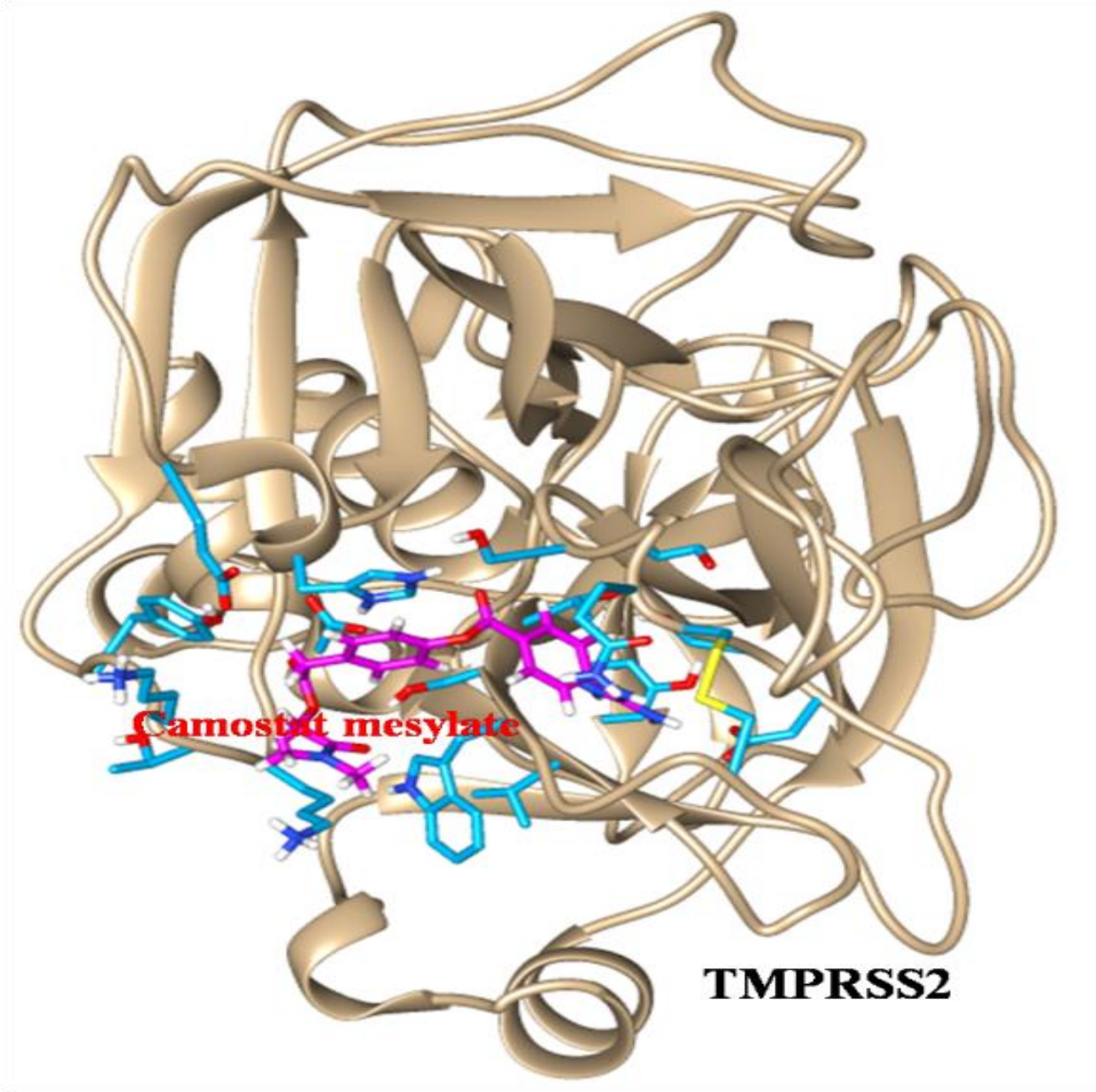

Supplementary figure 3: Docked complex of TMPRSS2 and Camostat mesylate complex obtained by online docking server.

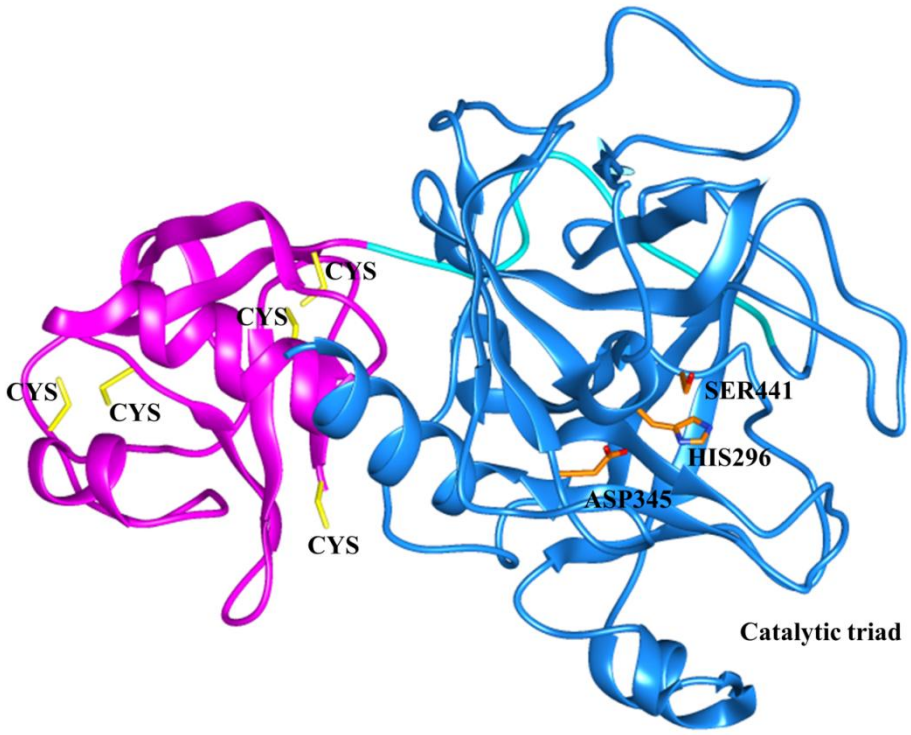

Figure 1: Predicted model of TMPRSS2 showing SRCR: Scavenger receptor cysteine rich domain (magenta) and catalytic triad HIS296, ASP345, and SER441 (orange) in serine protease domain (blue).

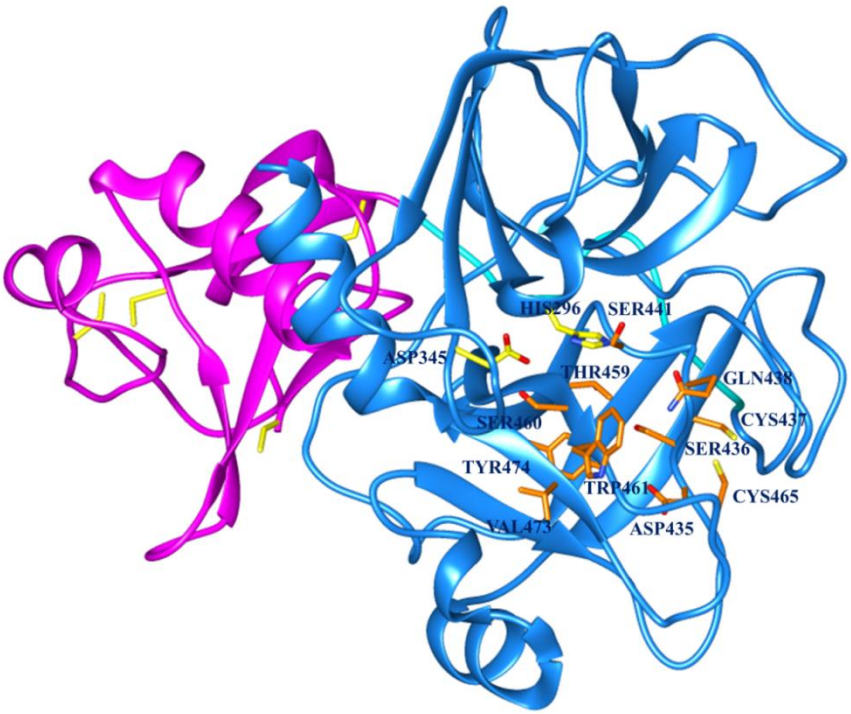

Figure 2: Predicted binding pocket by CATSp showing active site residues in orange.

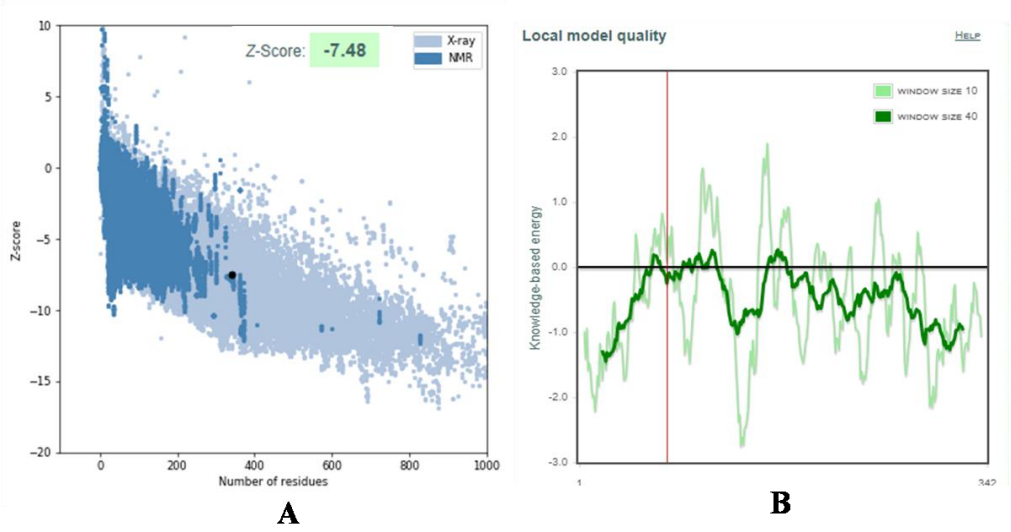

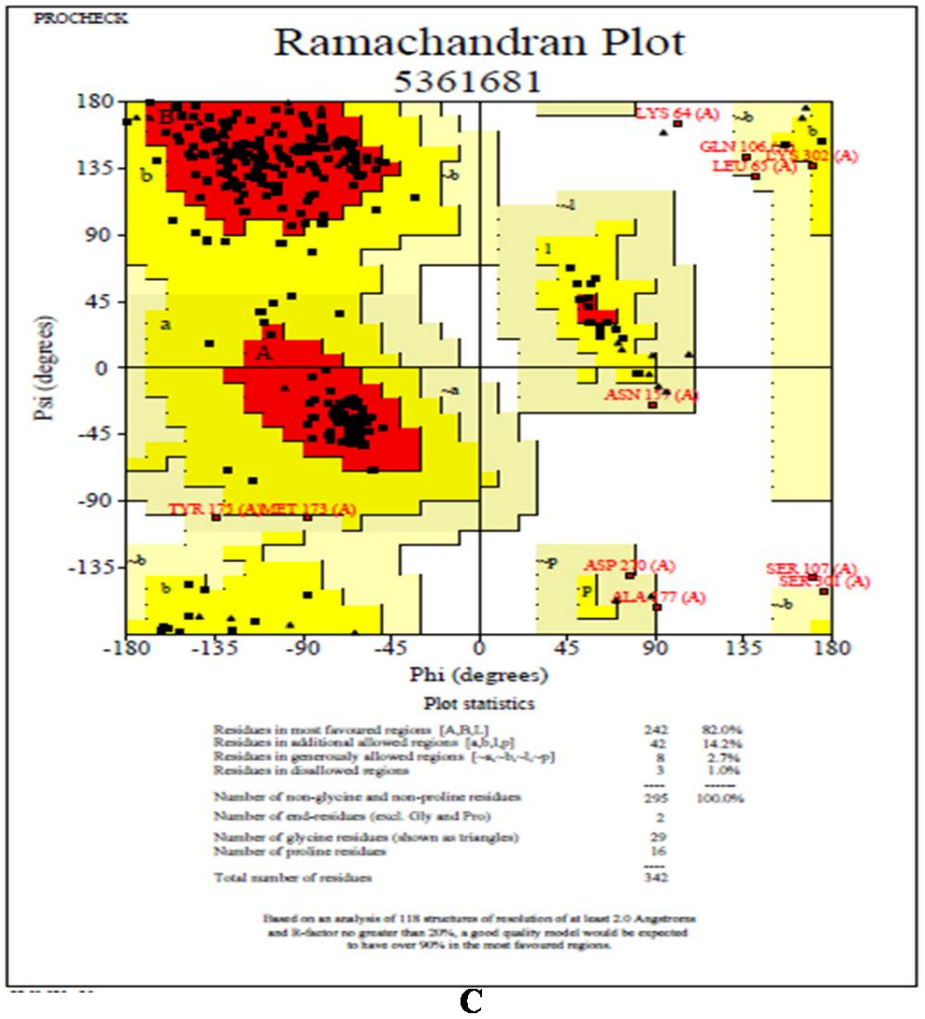

Figure 3: PROSA analysis of TMPRSS2 model A) Z Score, B) Local model quality. C) Ramchandran plot of TMPRSS2 model.

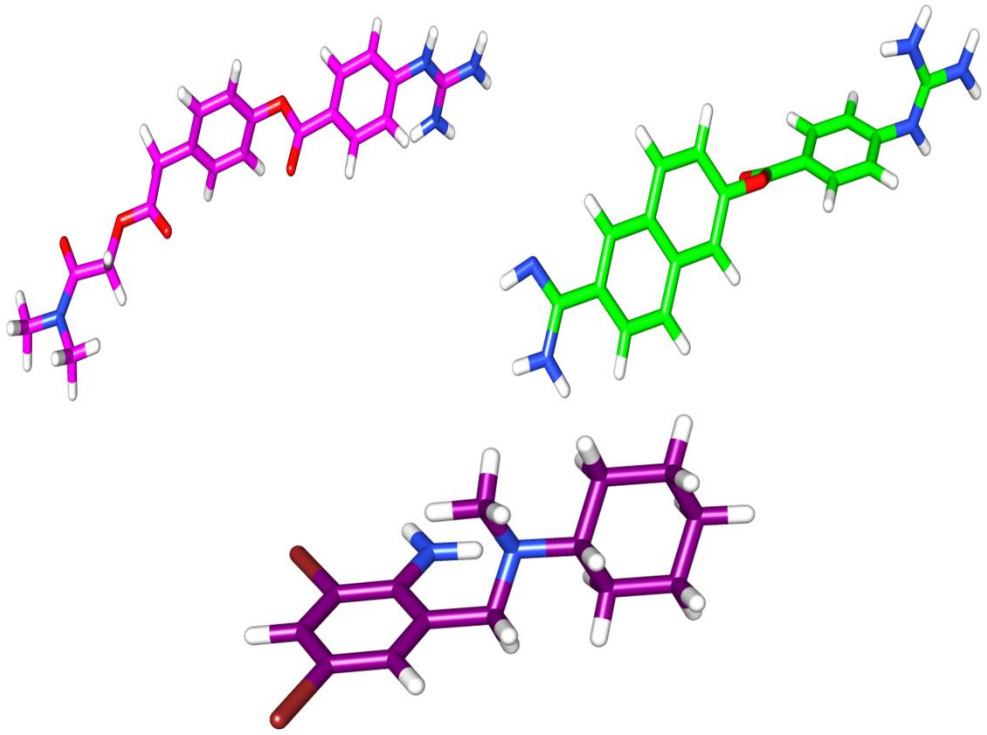

Figure 4: Three dimensional structure of TMPRSS2 inhibitors Camostat mesylate (Magenta:L1), Nafamostat (green:L2) and Bromhexine hydrochloride (purple:L3).

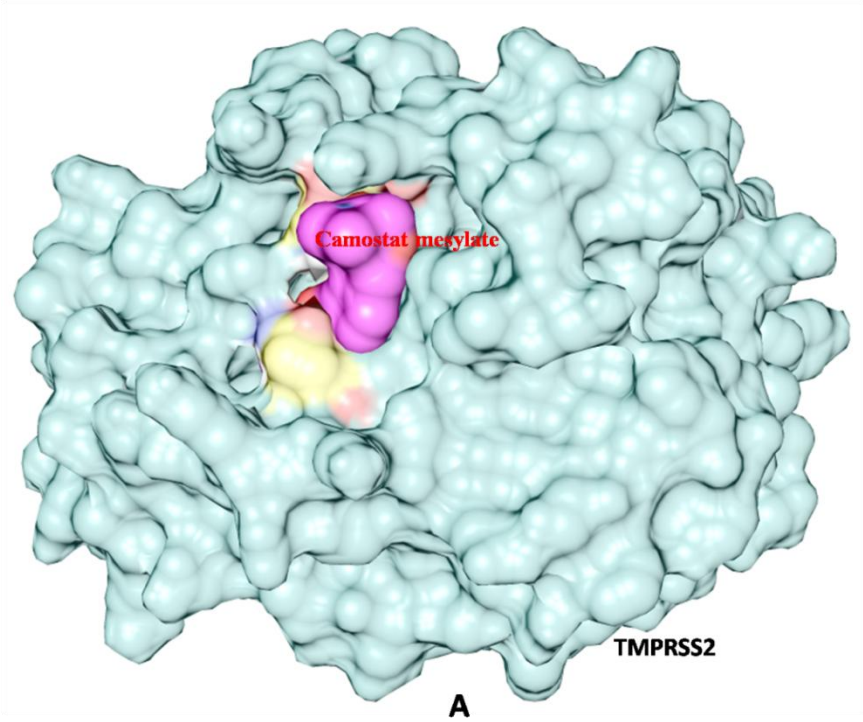

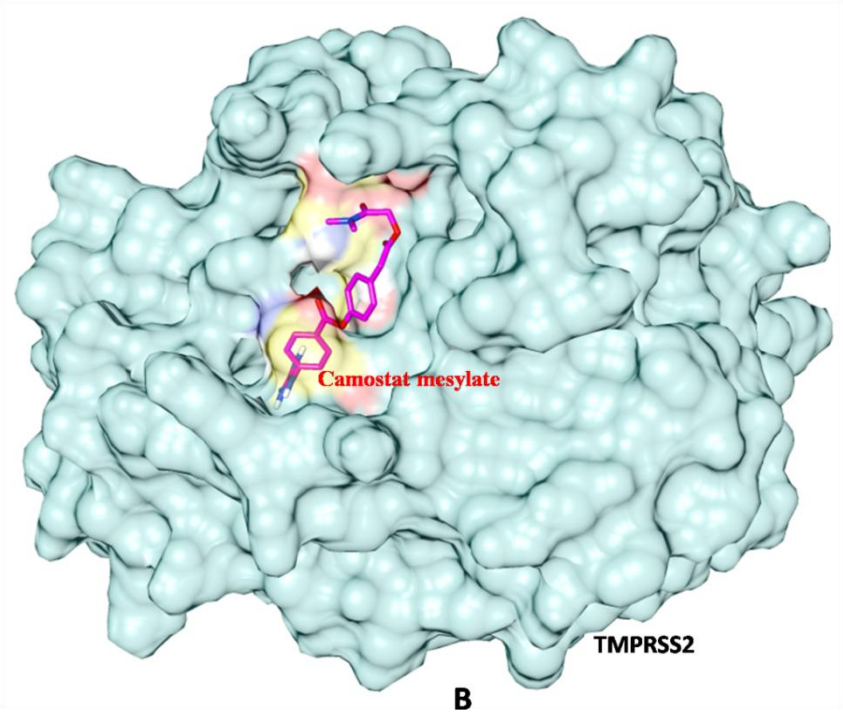

Figure 5: Binding of Camostat mesylate (Magenta) with TMPRSS2 (Light sea green) inside its pocket shown in surface (A) and Atoms/Bonds type (B). Binding of Camostat mesylate (Magenta) with active site residues (Yellow) of TMPRSS2 (Light sea green) inside its pocket shown in surface.

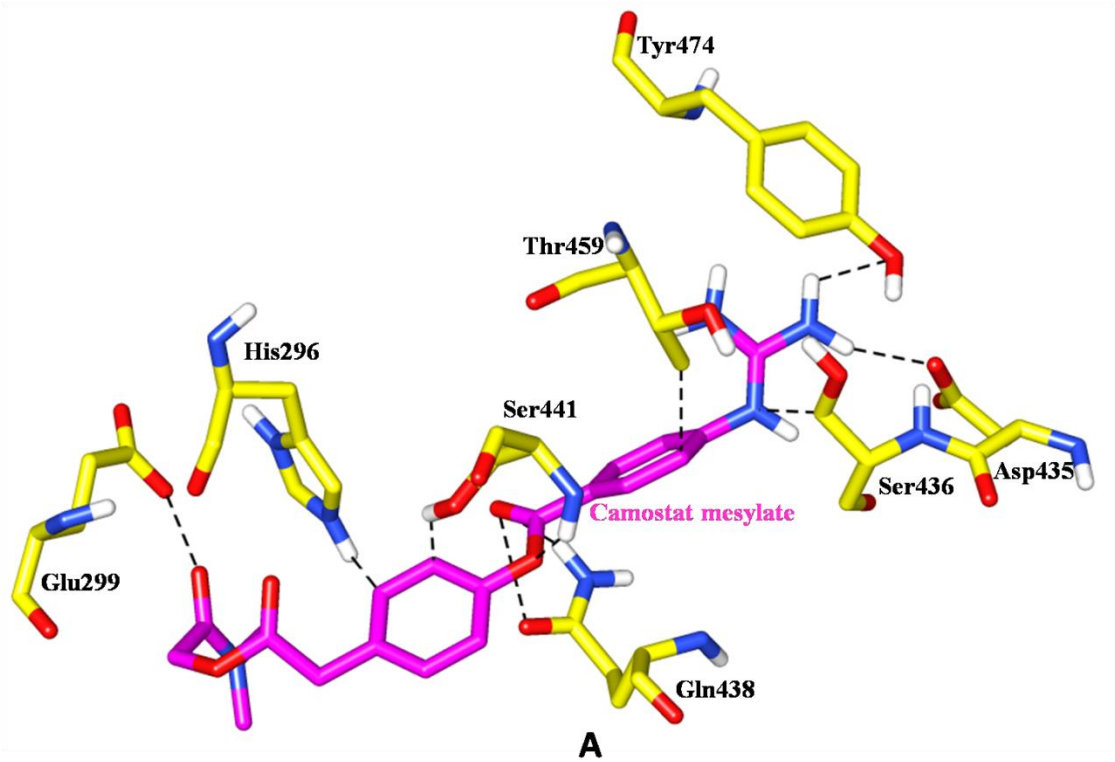

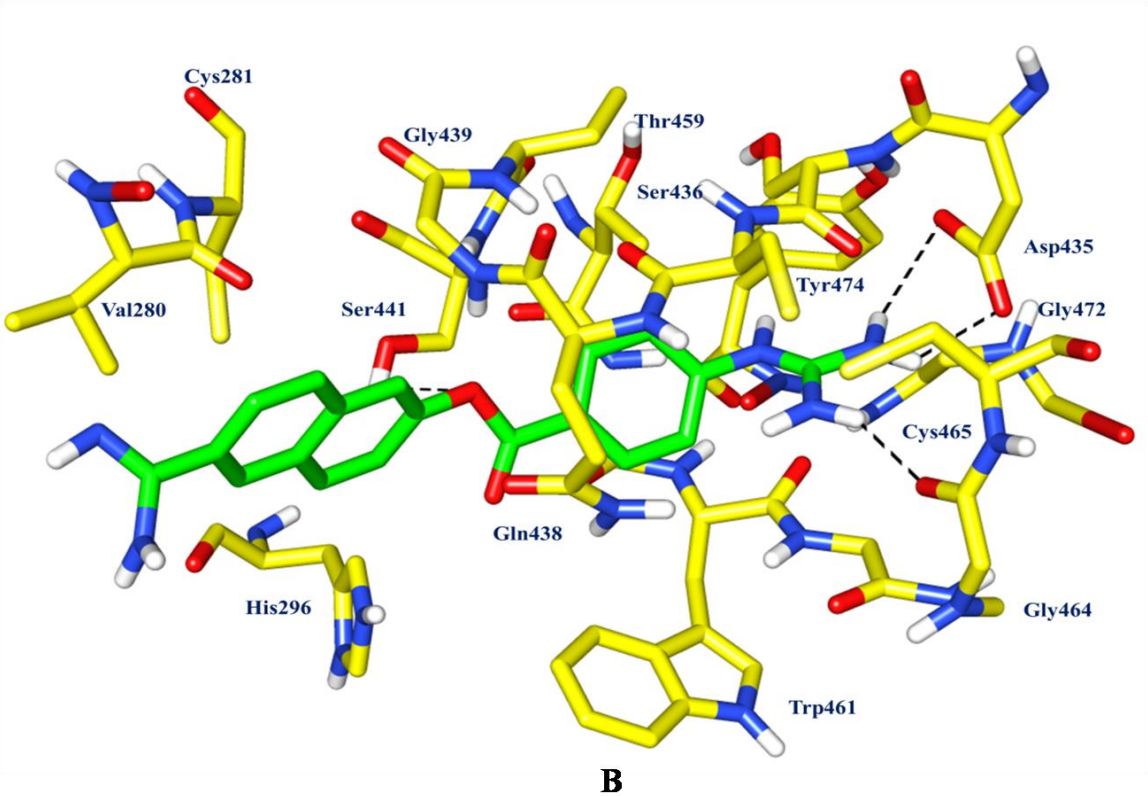
Cys281
Gly439
Thr459
Ser436
Asp435
Tyr474
Val280
Ser441
Gly472
Cys465
Gln438
His296
Gly464
Trp461

B

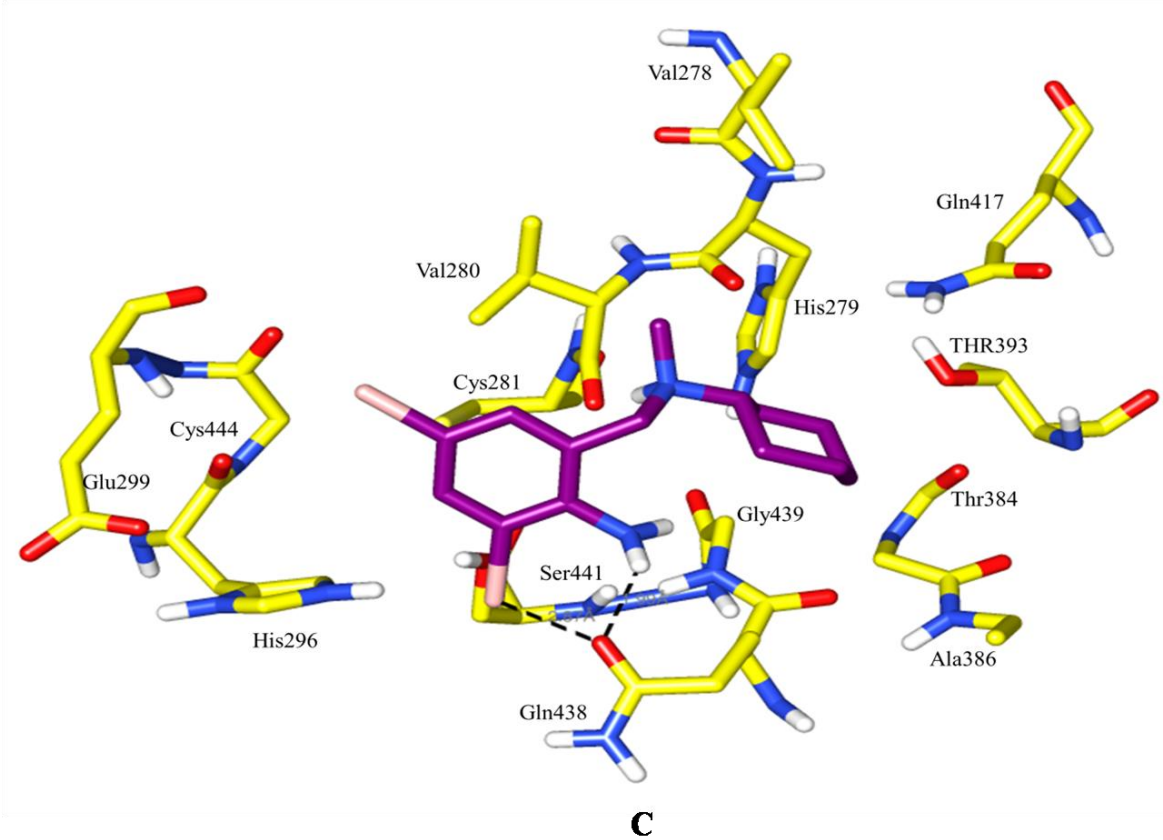
Val278
Gln417
Val280
His279
THR393
Cys281
Cys444
Glu299
Gly439
Thr384
Ser441
His296
Ala386
Gln438

C

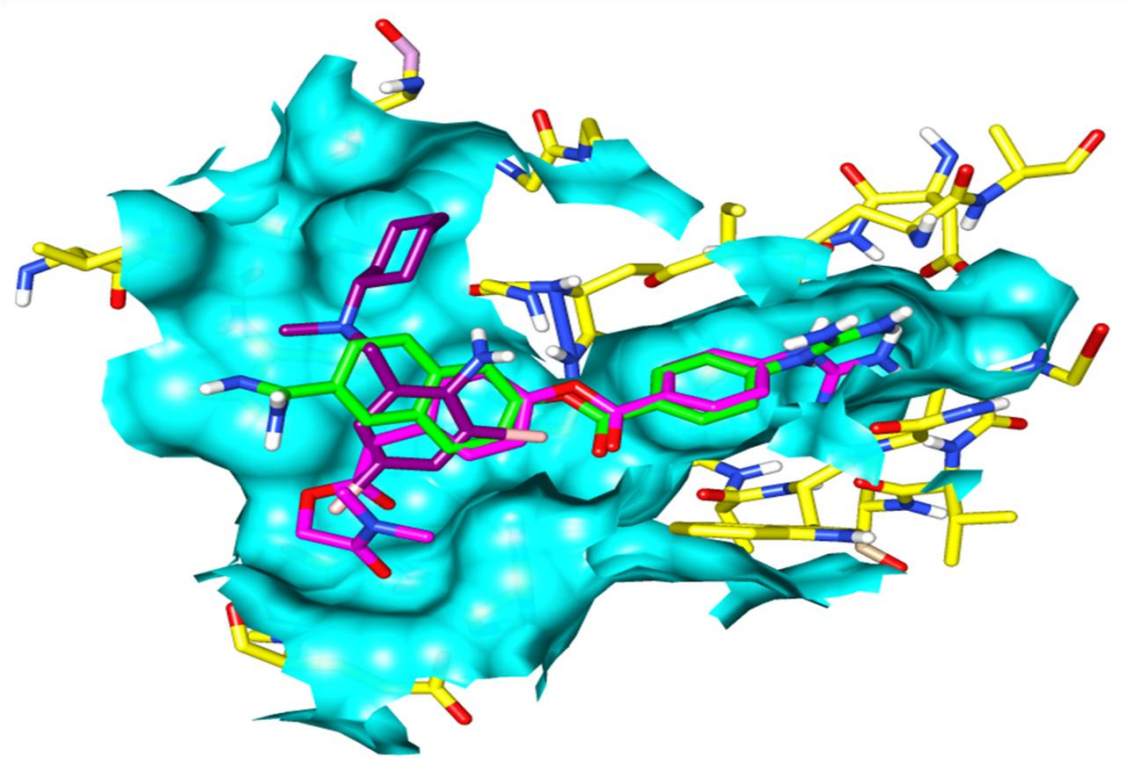

Figure 6: Docking interaction of active site residues of TMPRSS (Yellow) with A) Camostat mesylate (Magenta) B) Nafamostat (green) C) Bromhexine hydrochloride (purple) and showed in Atoms/Bonds type. D) Super imposition of docked complex of all three inhibitor showing Camostat mesylate (Magenta), Nafamostat (green) and Bromhexine hydrochloride (purple) within active site of TMPRSS2 active site residues (Yellow).